Elastic-Plastic Analysis of Base Mat Concrete for Base Isolated FBR

ISHIDA Katsuhiko, SHIOJIRI Hiroo
CRIEPI, Abiko, Japan
KONNO Takaaki, MORIYA Keiji
Kajima Corporation, Tokyo, Japan

ABSTRACT

As an item for study of building structures when introducing the isolation method to FBR, a review of the ultimate condition of the FBR isolation system inclusive of the base mat and isolation element was conducted, by the load increment method using the Finite Element Method (FEM) model. The results of analysis indicated that; the isolation layer and base mat both possessed sufficient strength; when the analysis was performed up to equivalent of 4 times the S_2 earthquake, the ultimate condition was produced in parts of the base mat, however, as a whole, sufficient strength remained; and the definite ultimate load could not be confirmed.

1 INTRODUCTION

As one of the research and development for the FBR commercial reactor of Japan, the study of FBR isolation system is being promoted for a period of seven years since 1987. By introducing the isolation system a rational earthquake resistant design can be realized in which the seismic incident can be reduced, making possible a considerable decrease in the thickness of the base mat in comparison with the conventional ones.

As one of the studies for a rational building structure when the isolation system is introduced to FBR, it was decided to analytically review the ultimate condition of the FBR isolation system inclusive of the building base mat and the isolation elements, in case the thickness of the base mat is made thinner, to find out such as; up to what extent of the earthquake load can the isolation layer maintain its integrity; the changes that will occur to loads that are applied to isolation element when cracks are produced in the base mat; and, which will attain ultimate condition first between the isolation element and the base mat.

SMiRT 11 Transactions Vol. K (August 1991) Tokyo, Japan,

2 ANALYSIS CONDITION

2.1 Analysis model

(1) Upper and lower base mat
The outline of the building used for the analysis is shown in Fig.1. The lower part of the building is supported by 276 isolation elements of rated weight of 500ton, and is so conceived to reduce the seismic incident to the upper building. The arrangement of the reinforcing steel bars were determined by elastic design for S_2 earthquake (Fig.2).

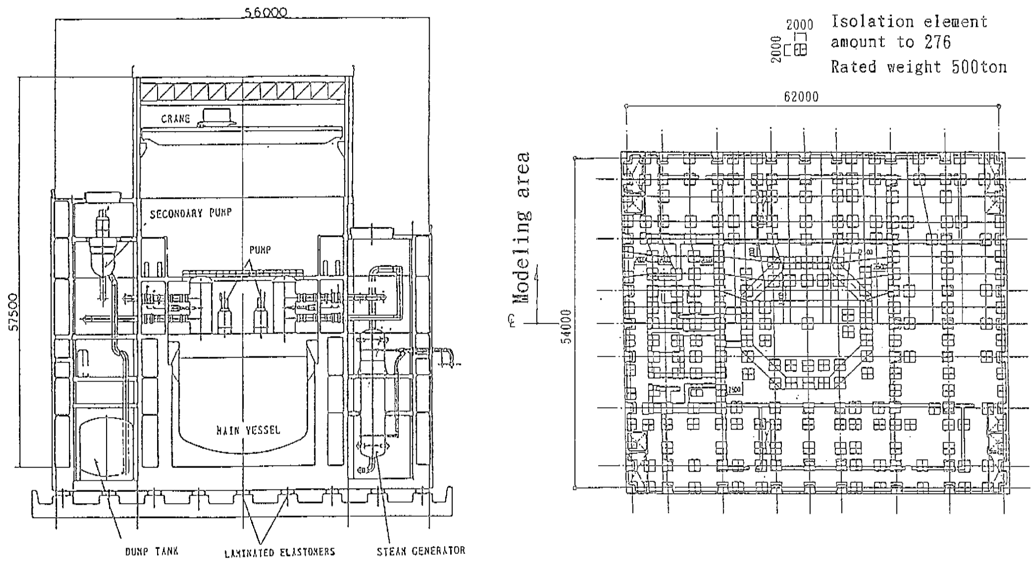

Section

Plot plan of the isolation rubbers

Fig.1 Plan and section of the base isolated FBR building

Upper mat

Lower mat

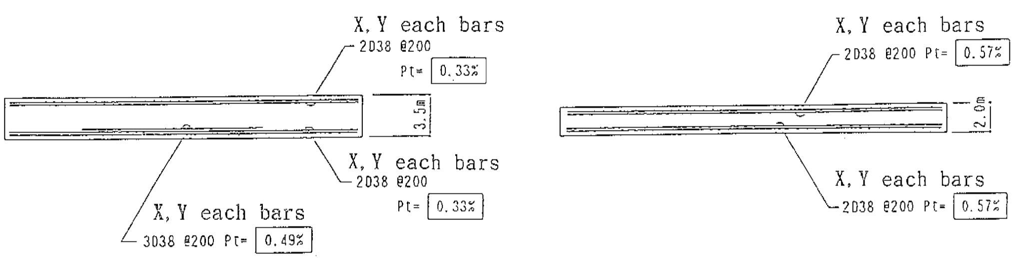

Fig.2 Reinforcement of the mat slab

Regarding the modeling for the building; for the base mats that are located at the top and bottom of the isolation elements, by the laminated shell element; and for the upper part from the base mat, by the beam element with considerations given to the stiffness of the shear wall (Fig.3). The laminated shell elements are divided in several layers in the direction of the plate thickness so that evaluations can be made of concrete cracks, compressive yield, compression failure and reinforcing bar failure. The non linear characteristics of the reinforcing bars were determined as shown in Fig.4.

(2) Isolation elements
The characteristics of the isolation element was established for analytical purpose from the test results of isolation element tests that were conducted as a part of this project. The load deformation characteristics and fracture curves of the isolation element are shown in Fig. 5.

(3) Ground
The supporting ground was assumed to be Vs = 1500m/s, and was modeled by 3 dimensional spring elements at each panel point of lower base mat. Each spring element was assumed to be independent and the lift up of non linearity was considered.

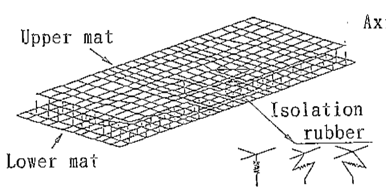

Fig.3 FEM Model

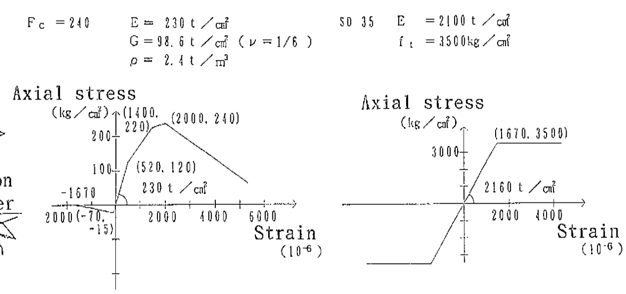

Concrete

Steel bar

Fig.4 Failure Models of the concrete and the reinforcement

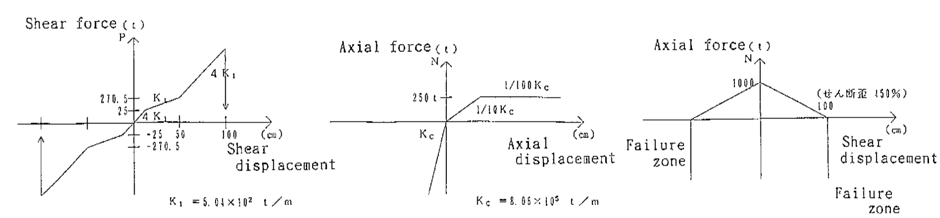

Shear force - displacement relationship

Axial force - displacement relationship

Failure interaction

Fig.5 Failure Models of the isolation rubber compressive force of the isolation element, appertained to the most outer edge on the compression side reached about 8 times of its own weight.

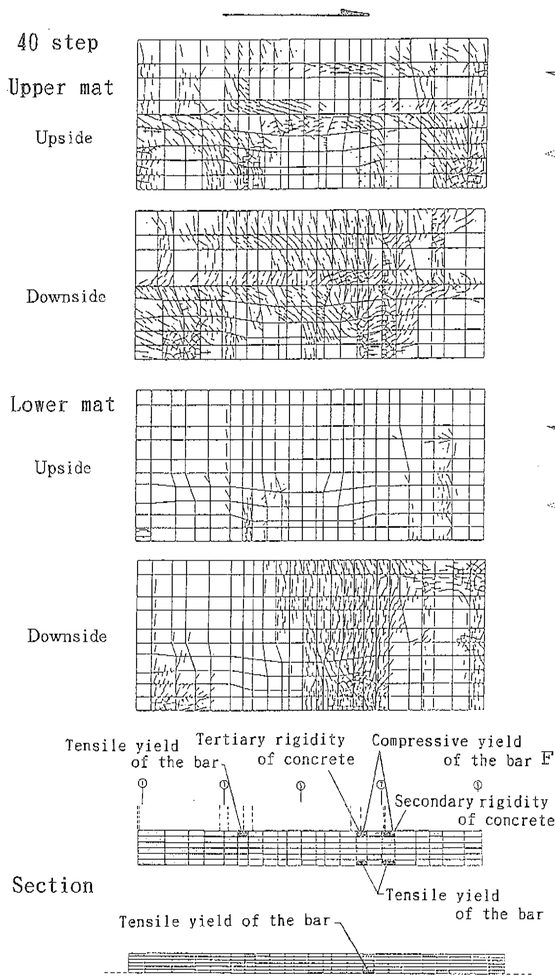

Fig.6 Analysed crack patterns of the mat slab

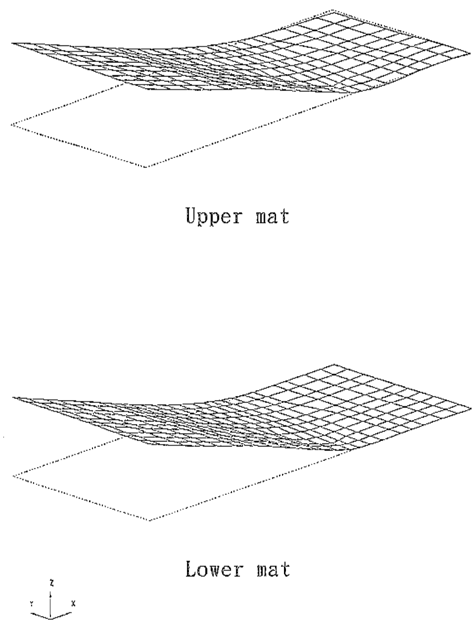

(Dead load + 4.0× S_2 load, 40 step)

Fig.7 Deformation of the mat slab

2.2 Loads

The basis of loads used for the analysis are the maximum response shear force and maximum response bending moment of each shear wall obtained by dynamic analysis of S_2 earthquake (i.e. rather long frequency component is considered and 1.5 times the tentative wave [M=8, Δ=50km, Mexico phase, α=328.5Gal] as determined by this project)(Table 1). The load for one step was 1/10 of S_2 earthquake load, and were applied by multiple proportions. For the analysis the vertical load was considered as step No. 0 and conducted until step No. 40 (Earthquake load equivalent to 4 times of S_2 earthquake).

Table 1 Maximum response shear force Q and maximum response bending moment M at the S_2 load

Location \ Response	Q (t)	M (tm)
Upper mat	42,830	102×10^4
Lower mat	50,070	112×10^4

3 ANALYSIS RESULTS

(1) Upper and lower base mats

Bending cracks appeared in the upper and lower base mats at the 10th step (at S_2 earthquake), tensile yield of reinforcing bars commenced at the 32nd step (3.2 times of S_2) and compressive yield of the reinforcing bars started at the 35th step (3.5 times of S_2). At the time the concrete had entered secondary rigidity, and reached tertiary rigidity at the 40th step (Fig.6).

Meanwhile, the lateral shear force of the upper and lower mats became the maximum at the border of the reactor support wall, and surpassed the lateral shear strength of concrete at the 15th step (1,5 times S_2).

The lower base mat showed partial uplift at the 10th step (at S_2) and the uplift expanded thereafter. At the 40th step (4 times S_2) the percentage that the total bottom surface came into contact with the ground area (contact ratio) became 29%, however, no disturbance was noted in deformation of the base mats (Fig.7).

(2) Isolation elements

Regarding the shear deformation of the isolation elements, at the 16th step (1.6 times S_2) almost all of the elements reached 50% of the shear deformation and entered the hardening range. As to the axial strength of the isolation element, tension commences to a part of the element at the 13th step, however, with approximately 200ton as the boundary the increase in tensile strength ceased, and entered a sideways move but did not reach fracture (Fig.8). This is because the weight of the lower base mat is considerably smaller when compared with the tensile strength of the isolation element, and with the increase in earthquake load the uplift of the lower base mat occurred. At the 40th and last step, the shear deformation of the isolation element reached 70% of the limit shear deformation. Also, the

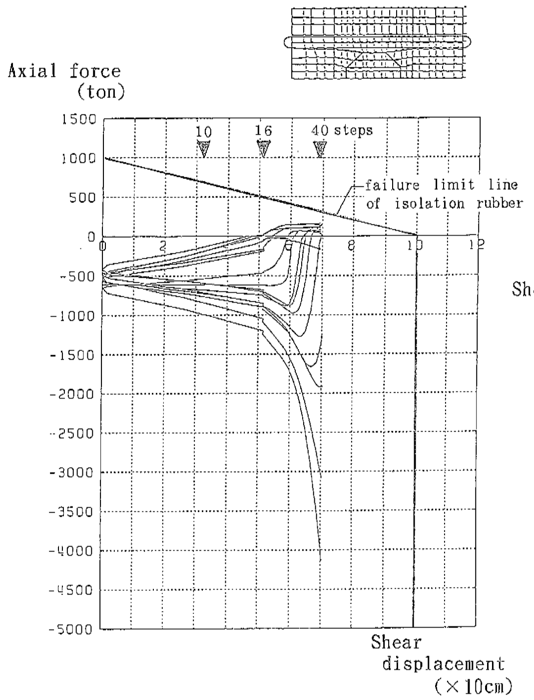

Axial force - shear displacement curves

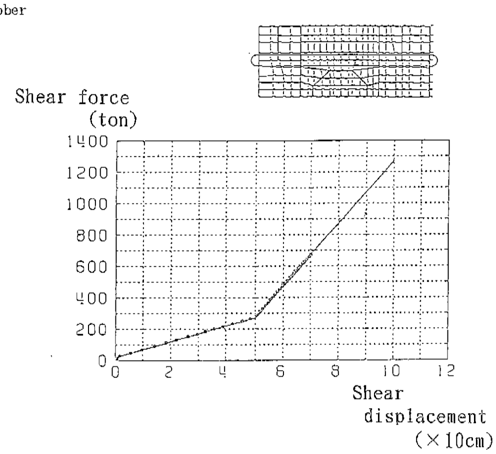

Shear force - shear displacement curves

Fig.8 Analysed force to displacement curves of the isolation rubbers

4 CONCLUSION

As the result of the analysis the isolation element did not reach fracture range relevant to the axial strength and shear deformation, and definite ultimate load could not be confirmed. However, it can be seen that the ultimate condition of the isolation system reaches the ultimate stage due to the strength of the base mat before the isolation element reaches fracture range, or the compressive strength of the isolation element, by the influence of the uplift of the base mat.
It was verified, however, that the isolation system has sufficient safety against S_2 earthquakes.

ACKNOWLEDGMENTS

This research is a part of a research project "Demonstration Test of Seismic Isolation System for Fast Breeder Reactor" sponsored by Ministry of International Trade and Industry.